International Journal of Applied Earth Observation and Geoinformation 14 (2012) 192–203

Contents lists available at SciVerse ScienceDirect

International Journal of Applied Earth Observation and Geoinformation

journal homepage: www.elsevier.com/locate/jag

Surface roughness analysis of a conifer forest canopy with airborne and terrestrial laser scanning techniques

K. Weligepolage[a,b,*], A.S.M. Gieske[a], Z. Su[a]

[a] Department of Water Resources, Faculty of Geo-Information Science and Earth Observation (ITC), University of Twente, Enschede, The Netherlands
[b] Department of Irrigation, P.O. Box 1138, Colombo, Sri Lanka

ARTICLE INFO

Article history:
Received 4 November 2010
Accepted 22 August 2011

Keywords:
Momentum roughness
Airborne laser scanning
Terrestrial laser scanning
Conifer forest

ABSTRACT

Two digital Canopy Height Models (CHMs) were generated using the novel Terrestrial Laser Scanning (TLS) technique combined with Airborne Laser Scanning (ALS) data, acquired over a conifer forest. The CHMs were used to extract cross-sections in order to derive surface geometric parameters. Different morphometric models were applied to estimate aerodynamic roughness parameters: the roughness length (z_0) and the displacement height (d_0). The CHMs were also used to derive the area–height relationship of the canopy surface. In order to estimate roughness parameters the observed canopy area–height relationship was modelled by uniform roughness elements of paraboloid or conical shape. The estimated average obstacle density varies between 0.14 and 0.24 for both CHMs. The canopy height distribution is approximately Gaussian, with average heights of about 26 m and 21 m for CHMs generated with data from TLS and ALS respectively. The estimated values of z_0 and d_0 depend very much on the selected model. It was observed that the Raupach models with parameters tuned to resemble the forest structure of the study area can be applied to a wide range of roughness densities. The cumulative area–height modelling approach also yielded results which are compatible with other models. The results confirm that, to model the upper canopy surface of the conifer forest, both the cone and the paraboloid shapes are fairly appropriate.

1. Introduction

Understanding the interaction between the Earth's surface and the lower part of the atmosphere is of paramount importance for many applications in meteorology, hydrology and related fields. It is known that this interaction is determined to an important extent by different exchange processes across the land atmosphere interface (Stull, 1988). One of the important exchange processes associated with the movement of air (wind speed) at the Earth's surface is the exchange of momentum (the product of mass and velocity of a volume of air). In the "free" atmosphere the movement of air is forced by the pressure gradient (difference in atmospheric pressure over a specified distance) resulting from differential solar heating of the surface and internal motion in the atmosphere. Once the moving air mass interacts with the surface of earth, the bottom layer is affected by the frictional forces (surface drag) acting against the motion. The surface drag acting on the bottom layer is transferred to the upper layers of the atmosphere by the internal stresses resulting in turbulence or irregular fluctuations in air motion. This entire process of momentum exchange at the surface of the earth is dominated by the surface roughness characteristic or the aerodynamic roughness.

Land surface models to estimate momentum exchange between the earth's surface and atmosphere often employ wind-profile relations above the surface using the flux-gradient approach or more specifically the relationship between momentum flux density (mass per unit area per unit time) and vertical gradient of wind speed above a surface (Garratt, 1992). However, the accuracy of model results depends much on the parameterization of aerodynamic roughness. Furthermore, the parameterization of aerodynamic roughness is important because it influences not only the momentum transfer, but also the exchange of heat, gases and aerosols across the earth. Parameterization of aerodynamic roughness has been done in hydro-meteorology by introducing two aerodynamic parameters: aerodynamic roughness length (z_0) and zero plane displacement height (d_0). The aerodynamic roughness length (also called momentum roughness length) is a surface length scale defined specifically by the logarithmic wind law for neutral conditions (Brutsaert, 1982). For homogeneous terrain under neutral conditions, the aerodynamic roughness length is the height at which the mean wind speed becomes zero, when extrapolating the logarithmic wind profile through the surface layer. When the wind

* Corresponding author at: Department of Water Resources, Faculty of Geo-Information Science and Earth Observation (ITC), University of Twente, P.O. Box 217, 7500 AE Enschede, The Netherlands. Tel.: +31 0 53 4874369; fax: +31 0 53 4874336.
E-mail address: weligepolage07078@itc.nl (K. Weligepolage).

1569-8432/$ – see front matter © 2011 Elsevier B.V. All rights reserved.
doi:10.1016/j.jag.2011.08.014

Nomenclature

b	Width of the frontal part of a roughness element (5 m)
c	Empirical coefficient (0.37)
c_1	Constant (1.09)
c_2	Constant (0.29)
C_S	Drag coefficient of the substrate surface (0.003)
C_R	Drag coefficient for an isolated surface-mounted roughness element (0.3)
c_{d0}	Drag coefficient at $z = h/2$ (0.3)
c_d	Constant (0.6)
c_{d1}	Free parameter (15)
d_0	Zero plane displacement height (m)
h	Mean canopy height (m)
h^*	Height of cone/paraboloid (m)
k	von Karman's constant (0.41)
u_h	Wind speed at $z = h$ (ms^{-1})
u_*	Friction velocity (ms^{-1})
z	Height above ground level (m)
z_0	Aerodynamic roughness length (m)
α	Fractional surface area
β	C_R/C_S
γ	(u_h/u_*)
γ_{max}	Constant value (0.3)
λ	Frontal area index
μ	Empirical stand specific constant (0.2–0.3)
ψ_h	Profile correction constant in the roughness sub layer (0.193)
τ_f	Form drag on the roughness elements per unit horizontal area
τ_s	Shear stress on the underlying substrate surface
τ_t	Total stress on the underlying substrate surface

blows over tall roughness elements like a vegetative canopy, there will be a vertical shift in the logarithmic form of the wind profile due to the surface roughness effects. The zero plane displacement height is the adjustment that has to be made in the measurement height due to this vertical shift from the ground surface. In physical terms, the displacement height is comparable to the level of action of the surface drag on the main roughness elements (Garratt, 1992). Using a semi-logarithmic plot of mean wind speed versus logarithm of height above the displacement height ($z - d_0$), z_0 may be graphically represented as the zero velocity intercept of the resulting straight line.

In general, roughness parameters are determined from micrometeorological or anemometric methods that use wind measurements by means of meteorological towers or balloon releases. Apart from anemometric methods, morphometric methods are also used. These methods use algorithms that relate roughness parameters to measurable dimensions of surface roughness elements. A review can be found in the literature (Hiyama et al., 1996; Grimmond and Oke, 1999; De Vries et al., 2003). Morphometric methods have distinct advantages over anemometric methods because they do not only avoid cumbersome measurements of meteorological variables but also allow estimation of roughness parameters for all wind directions. However, morphometric methods do have the disadvantage that they are mostly based on empirical relations and laboratory simulations and therefore require validation for natural environments.

Several studies were carried out recently to validate morphometric methods for different natural land surfaces. Hiyama et al. (1996) have evaluated algorithms to estimate regional roughness parameters of a complex landform with patches of various surface types. Grimmond and Oke (1999) have tested several morphometric methods to estimate aerodynamic parameters of urban landscapes. Menenti and Ritchie (1994) have computed the effective aerodynamic roughness in a complex landscape using airborne laser altimeter or LiDAR (Light Detection And Ranging) data to derive surface geometric features. Aerodynamic roughness of a natural forested area was determined with satellite imagery by Jasinski and Crago (1999) using Landsat images. Hasager et al. (2003) have used both Landsat and SPOT (Satellite Pour l'Observation de la Terre) images to estimate the aerodynamic roughness of a flat agricultural area with hedges. In a recent study, De Vries et al. (2003) have evaluated the use of laser altimeter data to extract surface geometric features of an area characterized by coppice dunes with interdunal areas partially covered with grass. More recently, Colin and Faivre (2010) estimated aerodynamic roughness length of landscapes ranging from dessert to grassland and irrigated farmland in the northwest of China from very high-resolution LiDAR data.

Although many surface types have been covered previously, few studies have used morphometric methods on surfaces dominated by forest canopies. However forests are complex ecosystems with unique characteristics and presently account for 30% of the global land area. Given the significant role of forests on the global energy and water balance, carrying out additional research to investigate aerodynamic roughness of such landscape is warranted. Particularly more attention should be paid to explore morphometric methods, those that employ state-of-the-art technology to determine aerodynamic roughness of forest surfaces. In order to develop operational methods to estimate forest aerodynamic roughness at regional scale, some improvements to existing methods are required. To be able to deal with large areas, the techniques should be computationally efficient and at the same time should produce results with a reasonable accuracy. In this regard progress can be made by adopting the recent advancement made in laser scanning techniques to map the upper canopy surface with a reasonable accuracy. When such detailed canopy surface maps are available, the method can be further refined by exploring new techniques to derive required surface morphometric parameters.

The aim of this study is to evaluate several morphometric methods to estimate the aerodynamic roughness of a region covered by forest. We adopted two different techniques to estimate surface morphometric variables of a densely vegetated terrain. We assumed that the upper canopy of a dense forest in principle acts as a spatially continuous impenetrable surface. Based on this assumption we digitally mapped the upper canopy surface which in turn was used to derive surface morphometric variables. One of the objectives of the study is to make use of a recently developed high resolution Terrestrial Laser Scanning (TLS) technique to digitally map the upper canopy surface through a multi-scanning approach including a range of different heights. Additionally, we used Airborne Laser Scanning (ALS) data to digitally map the canopy surface of the forest. Although the ALS technique is well established for large-scale canopy surface mapping (Hollaus et al., 2006), hardly any studies are known where this technique is applied to vegetative canopy surface roughness estimation (Menenti and Ritchie, 1994).

The structure of the paper is briefly outlined. Section 2 describes the study area and data used in the analysis, while Section 3 deals with existing models for estimating aerodynamic roughness and the methodology for generation of canopy height models. Sections 4 and 5 explain the two techniques adopted to derive surface morphometric parameters and subsequently discuss the results of different roughness models. Finally some concluding remarks are given in Section 6.

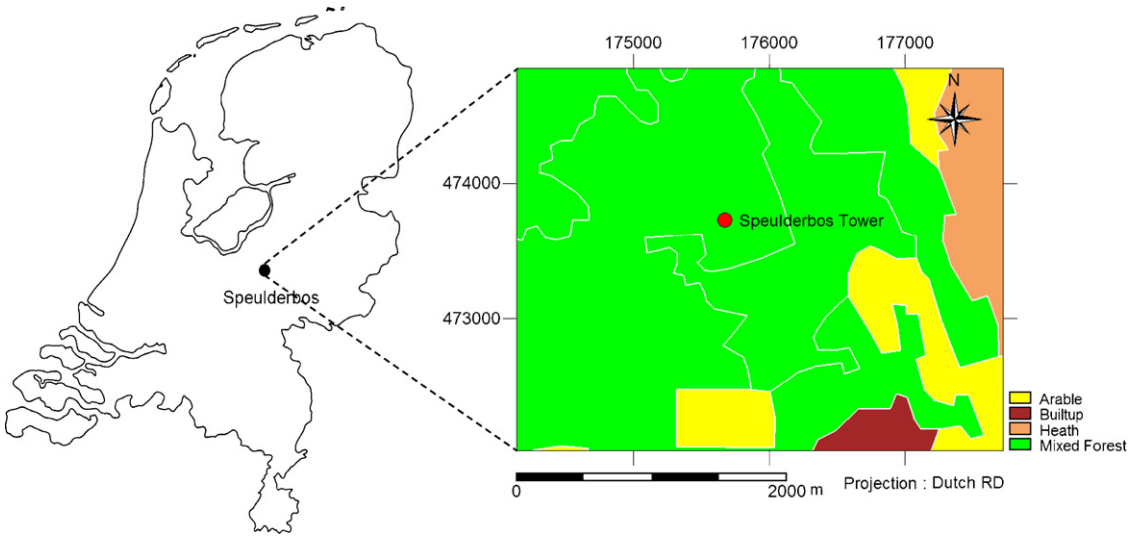

Fig. 1. Locations of the Speulderbos forest and the land cover distribution of the neighbouring area of the micro-meteorological tower site.

2. Background

2.1. Study area

During the EAGLE 2006 campaign in June 2006 extensive measurements of atmospheric boundary layer (ABL) variables were carried out at 3 locations in The Netherlands. One of the locations is the 46 meter high tower operated by the National Institute for Public Health and the Environment (RIVM) placed within a 2.5 ha Douglas fir (*Pseudotsuga menziesii*) stand within a large forested area (Speulderbos) in the central part of the Netherlands (see Fig. 1). The area has been extensively studied by many Dutch researchers (see e.g. Bosveld, 1999). The forest was planted in 1962, and stand density of 780 trees per hectare was reported in early nineties without a significant understory. Based on the 1993 observations, Dorsey et al. (2004) reported that there was a high degree of canopy closure with no tree foliage below 10 m. The single sided leaf area index (LAI) as reported in Bosveld (1999) based on a research carried out in 1991 is about 10 $m^2\ m^{-2}$. More recently, Van der Tol et al. (2009) reported an optical LAI of approximately 5 $m^2\ m^{-2}$ based on Photosynthetically Active Radiation (PAR) measurements above and below the canopy. The mean tree height which was about 22 m in early nineties, increased to 32 m in 2006. The surrounding forest stands have typical dimensions of a few hectares and varying tree heights. Dominant species in the neighbourhood of the Douglas fir stand are Japanese Lark (*Larix pinaceae*), Beech (*Fagus sylvatica*), Scotch Pine (*Pinus sylvestris*) and Hemlock (*Tsuga canadensis*). The vegetation consists of forest at distances of one to several kilometers. The topography of the study area is slightly undulating with elevation varying from 30 m to 50 m. Land cover data, originating from the Corine Land cover database (EEA, 1992), is available for the study area in the ArcView Shape format. Fig. 1 shows the dominant land cover classes in the study area.

2.2. TLS and ALS data

During the EAGLE 2006 campaign, a detailed 3-D representation of the Speulderbos forest site was obtained using the Leica HDS2500 pulsed laser scanner (Su et al., 2009). In order to obtain the 3D geometry of the canopy, the laser scanner was mounted

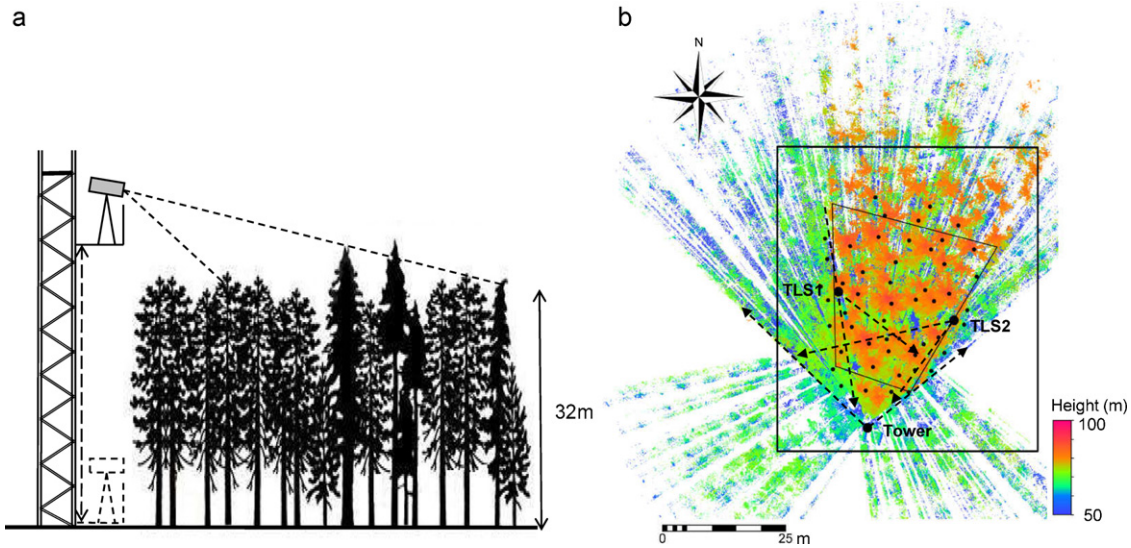

Fig. 2. Terrestrial Laser Scanning (TLS) at Speulderbos. (a) The scaffolding Tower and the vertical movement of the scanner. (b) The plan view from three directions (Tower and two ground locations TLS1, TLS2).

on the tower site elevator to scan at different heights and at two other ground locations. Fig. 2a shows the scan configuration of the TLS procedure. The instrument has a single-point range accuracy of ±4 mm, angular accuracies of ±60 μrad, and a beam spot size of only 6 mm from 0 to 50 m range, including point-to-point spacing as fine as 1.2 mm at 50 m. The data is available in ASCII .xyz format in the Dutch RD (Rijks Driehoeksmeting) system with reference to new Amsterdam zero level (NAP). The raw data was pre-processed to pixels of 10 by 10 cm and in each cell the maximum height was recorded. The colours in Fig. 2b show the resulting heights with respect to mean sea level. (For interpretation of the references to colour in this text, the reader is referred to the web version of the article.) The polygon shows the area used for the forest roughness analysis, while the rectangular area indicates the area used for the ALS analysis. Since TLS was performed at multiple levels by mounting the scanner to the elevator (Fig. 2a), reflected points below the forest canopy level (trunk-space) were also recorded as horizontal slices. By plotting the horizontally sliced points obtained from the trunk-space on the *x*–y plane, it was possible to locate the positions of the individual tree trunks. These have been indicated as small black dots in Fig. 2b.

AHN provides high density ALS data which describe the elevations of The Netherlands and the dataset is available through the product AHN-1. The raw data set used for this study has been acquired in year 2000 and contains the reflection of the laser beam on the vegetation, any manmade object present on the terrain or the ground itself. The terrain elevations have been obtained subsequently through a filtering procedure (Van Heerd et al., 2000). Both the raw data set (tree-top elevations) and the corresponding filtered dataset (terrain elevations) are available for the study area in the ASCII .xyz format with reference to the Dutch RD coordinate system. The terrain elevation dataset can be subsequently used to generate a digital terrain model (DTM) of the area.

3. Theory and methods

3.1. Some basic concepts and terminology

In principle rough surfaces can be categorized as either bluff-rough or permeable rough according to the respond of the roughness elements to wind flow (Brutsaert, 1982). A surface is called a bluff-rough surface when the roughness elements act as impermeable obstacles. A ploughed agricultural field, rigid vegetation like a cabbage plantation, an urban area closely packed with buildings are few examples for bluff-rough surfaces. However most of the natural surfaces consist of roughness elements which are permeable to wind, hence do not behave as bluff-rough surfaces.

For surfaces with large scale permeable roughness elements, the total stress (τ_t) exerted by turbulent boundary-layer flow is shared between the roughness elements and the underlying substrate surface and can be expressed as:

$$\tau_t = \tau_f + \tau_s \tag{1}$$

where τ_f is the form drag on the roughness elements per unit horizontal area and τ_s is the shear stress or the frictional force per unit area acting on the underlying substrate surface.

It is also important to differentiate the definitions used in forestry to describe the stand height of a forest canopy. The average tree-top height within a forest stand is defined as the arithmetic mean of individual tree heights usually measured in the field using equipments such as hypsometers and electronic total stations. Another definition adopted is the Lorey's mean height where the individual tree heights are weighted in proportion to their basal area. The canopy height which is more relevant to remote sensing studies is defined as the vertical extent of the vegetation canopy from the ground surface to the top of the canopy over a regular grid. Usually the canopy height is more in agreement with the Lorey's mean height.

3.2. Models to estimate roughness parameters

For bluff-rough surfaces, Kutzbach (1961) proposed the following empirical relationship to estimate d_0.

$$\frac{d_0}{h} = c_1 \lambda^{C_2} \tag{2}$$

λ is the obstacle density defined as the ratio sn/A where s is the cross sectional area of the obstacle measured in a vertical plane perpendicular to the wind direction, and n number of obstacles on a horizontal area A. The constants c_1 and c_2 were determined by Kutzbach (1961) as $c_1 = 1.09$ and $c_2 = 0.29$ for a simulated bluff-rough surface.

Grant and Mason (1990) incorporated the concept of total stress and proposed the following equation to calculate the effective roughness of complex terrain.

$$z_0 = \frac{h}{2} \exp\left[\frac{-k}{((0.5 c_{d0}\lambda + k^2)/(\ln^2(h/2z_{01})))^{0.5}}\right] \tag{3}$$

where k is the von Karman's constant taken as 0.41, z_{01} is the local roughness length representing the shear stress component of the substrate surface and c_{d0} is the drag coefficient at $z = h/2$. For bluff bodies the value of c_{d0} varies between 0.2 and 0.8 depending on the shape of the obstacles (Mason, 1985). A value of $c_{d0} = 0.3$ was used by Grant and Mason (1990) to calculate the effective roughness length of an area of sinusoidal orography.

Using dimensional analysis and two physical hypotheses, Raupach (1992) developed a drag partition model and proposed a relationship to estimate momentum roughness length. Raupach's model considers not only the shelter effect of roughness elements on the substrate surface, but also that on the surrounding elements and proposed the following equation;

$$\frac{z_0}{h} = \left(\frac{h - d_0}{h}\right) \exp(\psi_h) \exp(-k\gamma) \tag{4}$$

where ψ_h is taken here as a profile correction constant equal to 0.193 (Raupach, 1995).

The parameter γ is the ratio (u_h/u_*) which is given by the following equation.

$$\gamma = (C_S + C_R\lambda)^{-1/2} \exp\left(\frac{c\lambda\gamma}{2}\right) \tag{5}$$

in which u_h is the wind speed at $z = h$, u_* is the friction velocity which is defined as the square root of the kinematic momentum flux $(\tau/\rho)^{1/2}$ where τ is the Reynolds' stress and ρ is the air density, C_S (taken as 0.003) is the drag coefficient of the substrate surface, C_R (given as 0.3) is the drag coefficient for an isolated surface-mounted roughness element, and $c \approx 0.37$ is an empirical coefficient. Since (5) is an implicit equation specifying γ as a function of λ, in general a solution is obtained numerically. The method of fixed point iteration (Burden and Faires, 2010) has been used here to estimate γ using (5).

Raupach (1992) also proposed the following model to estimate the displacement height.

$$\frac{d_0}{h} = \frac{\beta\lambda}{1 + \beta\lambda}\left[1 - c_d\left(\frac{b}{h\lambda}\right)^{1/2}\frac{1}{\gamma}\right] \tag{6}$$

where $\beta = C_R/C_S$, b is the width of the frontal part of a roughness element (here taken equal to 5.5 m), and c_d is a constant found to be around 0.6.

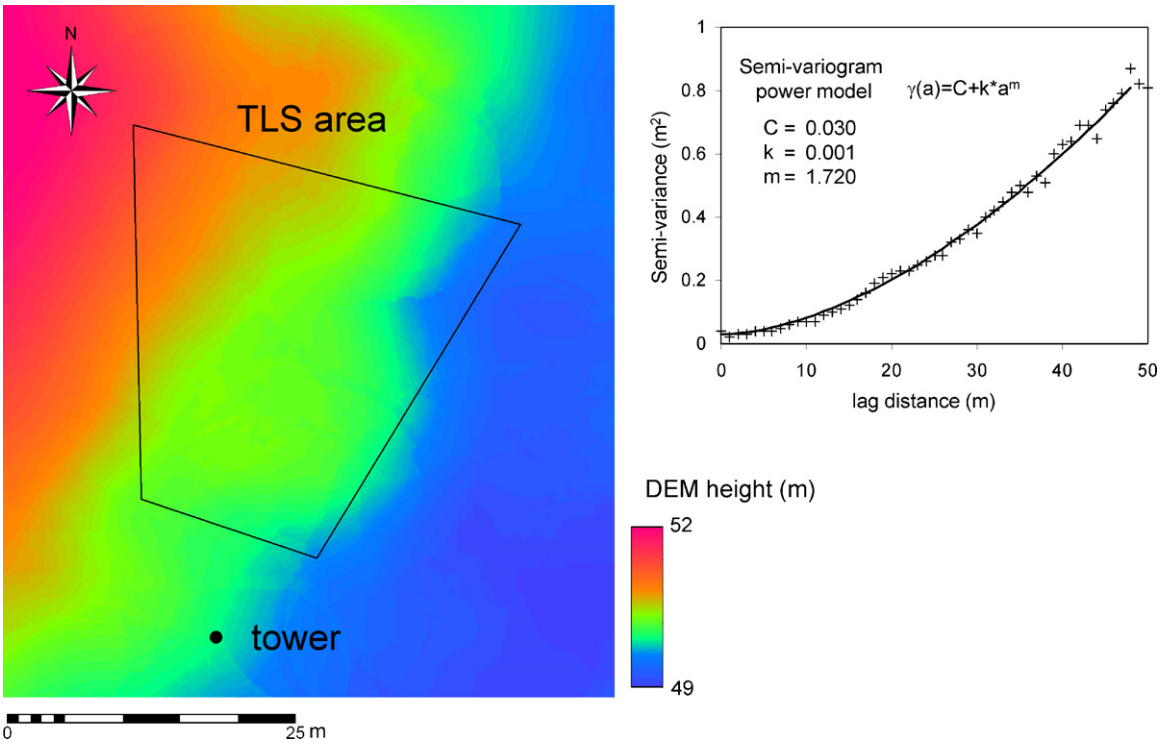

Fig. 3. Digital Elevation Model created by interpolating the ALS terrain elevation data and the power semi-variogram model used for ordinary kriging.

Raupach (1994) derived a simple analytical expression for roughness length of vegetated surfaces. Rather than using the full iterative solution of (5) for γ he proposed the following approximation equation for all $\lambda < \lambda_{max}$ which is about 0.3.

$$\frac{u_*}{u_h} = \min\left[(C_s + C_R\lambda)^{1/2}, \left(\frac{u_*}{u_h}\right)_{max}\right] \quad (7)$$

where $(u_*/u_h)_{max}$ is a constant value of about 0.3, when $\lambda > \lambda_{max}$ (which is also about 0.3).

The simplified approach of Raupach (1994) is given as

$$1 - \frac{d_0}{h} = \frac{1 - \exp(-\sqrt{2c_{d1}\lambda})}{\sqrt{2c_{d1}\lambda}} \quad (8)$$

where c_{d1} is a free parameter found to be around 7.5 by fitting (8) to observed values.

3.3. Generation of canopy height models (CHM)

The first step towards the generation of CHM is the generation of the DTM of the area. In order to generate the DTM we used a geo-statistical method (ordinary kriging) by which the irregularly spaced ALS terrain data points with *x*, *y*, *z* coordinates were interpolated. First the experimental semi-variogram was calculated using the ALS terrain elevation points and fitted with a power semi-variogram model as shown in Fig. 3. Using the power semi-variogram model, point data was interpolated through ordinary kriging. The resulting DTM, resampled to a resolution of 10 cm × 10 cm, is also shown in Fig. 3. The DTM was subsequently used for generating canopy height models with both the ALS and TLS canopy elevation data sets as described in the following paragraphs.

Before further processing we made a comparison of canopy heights derived using the TLS and ALS raw data sets. This comparison made it possible to setup threshold values for minimum canopy heights and thereby to eliminate possible erroneous (low occurring) canopy height values present in both data sets. First using the pre-processed TLS raw data set with elevations for every 10 cm × 10 cm pixel, a polygonal area was selected for further analysis (see Fig. 2b). Then the ALS data set was used to select the canopy elevation points contained within that polygonal area. These points were subsequently used to extract the corresponding height values from the TLS raw data set. This was done using a GIS software by overlaying the point data from ALS on the raster image of TLS data. For each ALS point the corresponding elevation was obtained from the TLS image using few GIS operations. The corresponding terrain elevations for these data points were also obtained by repeating the same exercise using the previously generated DTM. The canopy heights for both the ALS and TLS data points were calculated by subtracting the terrain elevation from the respective canopy elevations.

The resulted canopy height data set of 226 points is shown in the scatter diagram of Fig. 4a, and as histograms in Fig. 4b. Fig. 4b shows the apparent canopy height difference between the TLS and ALS points. Moreover Fig. 4a and b show the occurrence of low canopy values for both TLS and ALS data. Fig. 4a was subdivided in 4 quadrants by a horizontal and a vertical line to illustrate the situation. The upper left quadrant shows the situation where TLS records are high and ALS records are low. Apparently, the ALS laser beam has penetrated through gaps in the forest canopy. This mainly depends on the laser footprint size and the canopy closure. The lower right quadrant shows high ALS and low TLS values. The differences may be due to errors in coordinates, or due to obstacle shadow effects. In view of the fact that the study area is characterized by rather dense canopies, it was decided to compensate for these discrepancies by only allowing TLS values greater than 15 m and ALS values greater than 10 m, i.e. restricting the data to the upper right quadrant of Fig. 4a. Fig. 5 shows the histogram for the entire TLS raw data set, illustrating the bimodal nature of the data with distinct peaks at about 2 m and 28 m. The threshold value of 15 m will effectively remove the lower part of the histogram.

Once the threshold values were identified, canopy surface data sets were further processed in the following manner. For the entire set of ALS data points the canopy heights were computed by

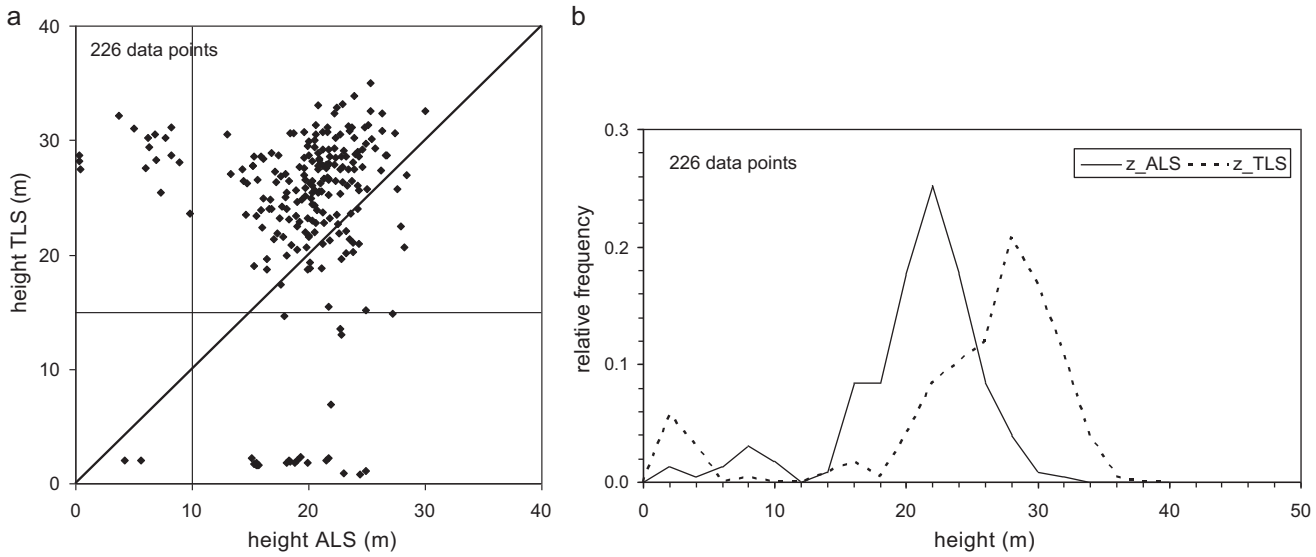

Fig. 4. Correlation between TLS and ALS canopy heights for 226 data points (a) and histograms of TLS and ALS canopy heights – bin size 2 m (b).

subtracting terrain elevations from the canopy elevations. From the computed canopy height data set, all the points with canopy heights below 10 m were eliminated. The resulted ALS canopy height data set was then interpolated on a grid of 10 cm by 10 cm using an exponential semi-variogram model (Fig. 6a) with nugget 7 m^2, sill 10.3 m^2 and range 3.5 m. Next, the ALS data was also interpolated with nugget zero (Fig. 6b). The resulted canopy height models (ALS-CHM) were shown in Fig. 6a and b. The processing of the TLS data set involved more steps. First, the raw canopy height model was obtained by subtracting the DTM values from the canopy surface elevations. Next, the pixels with raw canopy heights less than 15 m were removed. These gaps were then filled by inverse distance weighing (IDW) (Fig. 7a). Finally, a median 5×5 filter was applied to smooth the image as shown in Fig. 7b.

4. Estimation of roughness parameters using the CHM models

The CHM provides gridded three dimensional (3-D) information of the upper canopy surface. We adopted two different approaches to derive surface geometric parameters. In the first approach (described in this section), several cross-sections extracted from the CHM were used to derive obstacle density and mean canopy height. These surface features were then used to determine the roughness parameters with the algorithms described in Section 3. In the second approach (see Section 5), the observed area–height relationship of the CHM was modelled with basic geometric shapes.

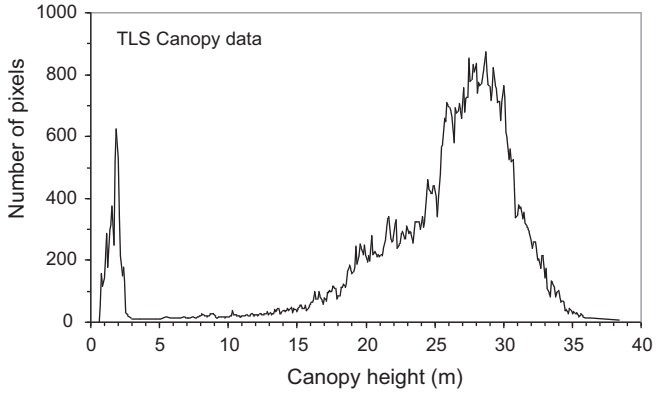

Fig. 5. Histogram of entire TLS canopy data set (bin size 1 m) showing bimodal character.

4.1. Estimation of obstacle density (λ) and mean obstacle height (h)

In the analysis we applied the algorithms of Grant and Mason (1990), Raupach (1992, 1994) and Kutzbach (1961) to estimate roughness length and displacement height. We calculated obstacle density λ using a method previously adopted by Hiyama et al. (1996) and De Vries et al. (2003). The method basically assumes that the surface is isotropic and the areal roughness density λ can be defined over a cross-sectional line as follows:

$$\lambda = \frac{\sum_{i=1}^{n} \Delta y_i}{\sum_{i=1}^{n} \Delta x_i} \quad \text{for } \Delta y_i > 0 \tag{9}$$

where Δy_i is the positive height difference for each Δx_i in the cross section.

In order to estimate surface features we extracted several cross-sections (height at 10 cm intervals) along North-South direction and East-West direction from the generated CHMs. The length of North-South TLS profiles are 30 m on average whereas the length of East-West profiles varies between 20 m and 25 m. The distribution of selected profiles is shown in Fig. 7a and b. The ALS profiles were taken along the same lines as shown in Fig. 7a and b but extended to the full length and width of the ALS canopy area (Fig. 6). The average profile height was estimated from the height values at 10 cm horizontal resolution along the profile.

In order to calculate obstacle density we adopted the procedure described by De Vries et al. (2003). First, the height values were smoothed by block averaging using intervals of 10 measurements. Subsequently, a moving average with a variable number of measurements was applied to the block averages to reduce random and system noise present in the laser measurements. Obstacle density was computed by integrating positive height changes divided by the distance using (9). To determine the correct moving average, λ versus the number of measurements in a moving average was plotted in Fig. 8. The figure shows three curves: (a) the curve derived from the TLS-CHM shown in Fig. 7a. The curve derived

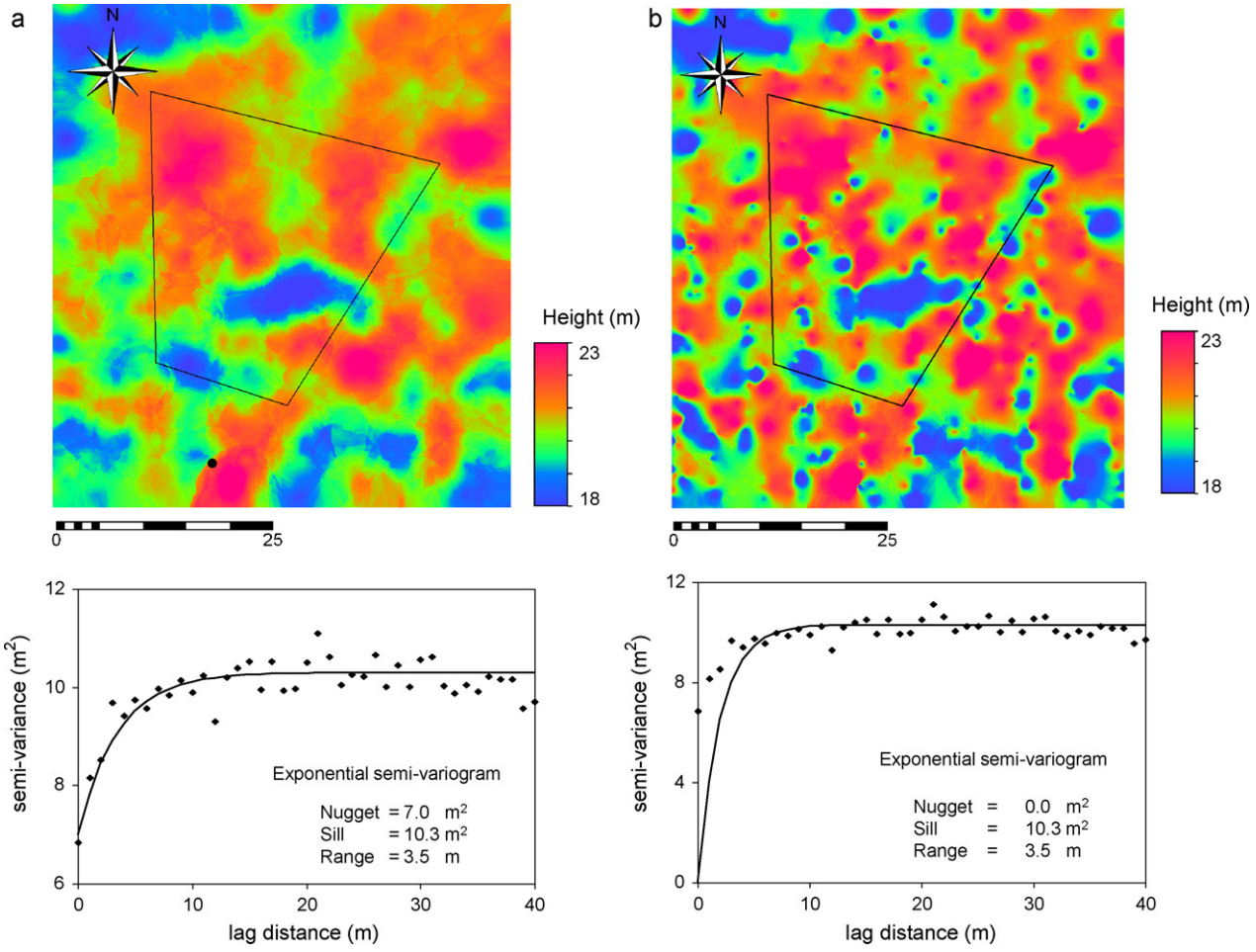

Fig. 6. ALS Canopy Height Models interpolated by ordinary kriging with the exponential semi-variogram models with Nugget 7 (a) and Nugget 0 (b).

from Fig. 7b is not shown because it is very much the same as the one derived from Fig. 7a. (b) The curve derived from Fig. 6b (nugget zero) and (c) the curve from Fig. 6a (nugget 7). The curves decline rapidly at low numbers and less rapidly at higher numbers and converge at around a number of 7 measurements in an average, as was reported also by De Vries et al. (2003). The procedure was repeated for all 10 profiles (5 N-S and 5 E-W) to obtain a spatial average value for the areal roughness density of the represented

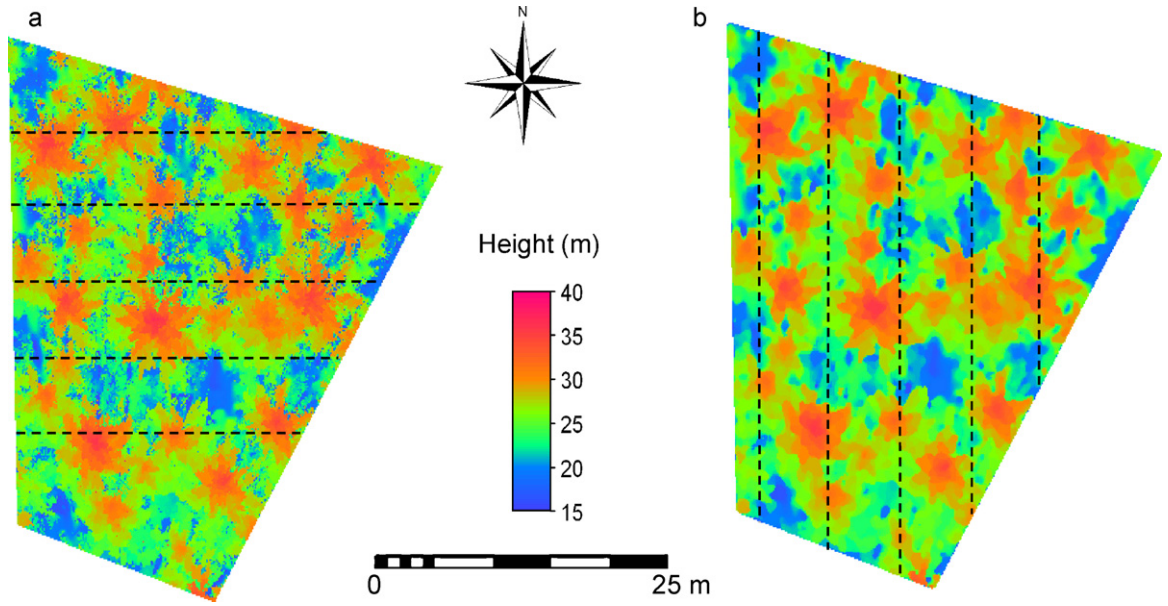

Fig. 7. TLS Canopy Height Models. (a) Gaps filled by IDW and (b) Running a Median filter (5 × 5 pixels). The dashed lines indicate the distribution of transects for two principal directions.

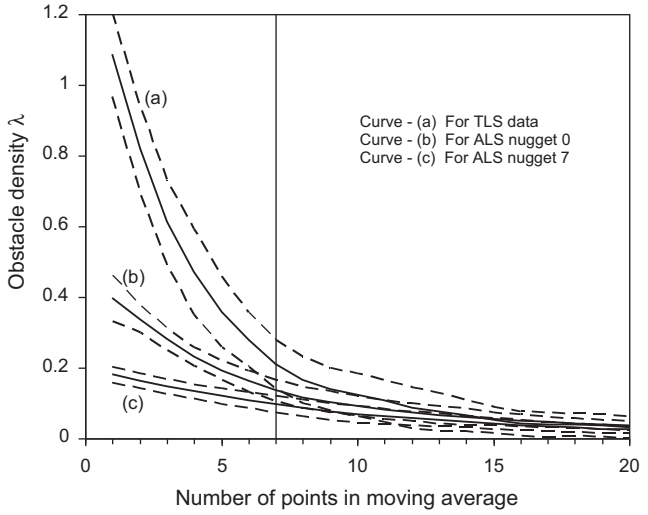

Fig. 8. Plot of the average obstacle density versus moving average number. Solid lines indicate the mean λ values for 10 profiles. Dashed lines show the range of λ for each curve.

Table 1
Statistical Summary of TLS-CHM derived canopy surface features for different directions.

Direction	Parameter	Average	Stand. Dev.
TLS_IDW			
N-S	λ	0.242	0.043
	h (m)	25.89	0.70
E-W	λ	0.179	0.067
	h (m)	25.72	1.49
TLS_M5			
N-S	λ	0.242	0.043
	h (m)	26.02	0.66
E-W	λ	0.174	0.065
	h (m)	26.00	1.62

Table 2
Statistical summary of ALS-CHM derived canopy surface features for different directions.

Direction	Parameter	Average	Stand. Dev.
Nugget 7			
N-S	λ	0.098	0.014
	h (m)	20.86	0.44
E-W	λ	0.096	0.028
	h (m)	21.10	0.41
Nugget 0			
N-S	λ	0.136	0.020
	h (m)	20.89	0.62
E-W	λ	0.136	0.036
	h (m)	21.28	0.42

canopy area. This resulted in 10 different sets of values for λ and h for the profiles extracted from each CHM. The statistical summary of the derived surface parameters are listed in Tables 1 and 2 and the range in values is also indicated in Fig. 8 by dashed lines. Table 3 summarizes the average canopy heights and obstacle densities derived for the three curves of Fig. 8. It is thought that the spatial interpolation of the ALS data with nugget 0 (Fig. 6b) reflects the real canopy surface better than the interpolation with nugget 7 (Fig. 6a). Interpolating with a high nugget value will smooth the canopy excessively. For this reason the roughness values are calculated based on curves (a) and (b) shown in Fig. 8.

Table 3
Summary of results for spatially average canopy height and obstacle density.

Method	h_{avg} (m)	λ (at $n = 7$)
TLS	25.81	0.2106
ALS nugget 7	20.98	0.0969
ALS nugget 0	21.09	0.1361

Table 4
Estimated roughness parameters using original model parameters.

Model	Average from TLS		Average from ALS	
	z_0 (m)	z_0/h	z_0 (m)	z_0/h
Grant and Mason (1990)	1.436	0.056	0.743	0.06
Raupach (1992)	0.751	0.029	0.548	0.03
Raupach (1994)	2.974	0.115	1.921	0.12

Model	Average from TLS		Average from ALS	
	d_0 (m)	d_0/h	d_0 (m)	d_0/h
Kutzbach (1961)	17.91	0.694	12.89	0.611
Raupach (1992)	21.60	0.837	16.81	0.797
Raupach (1994)	13.74	0.532	9.87	0.468

The individual profile details revealed that the roughness density and the average height estimates vary slightly between the extracted profiles. The spatial average values of Table 3 (i.e. TLS data and ALS data with nugget zero) were used for the roughness calculations and the obtained results are summarized in Table 4. The difference in average canopy height of the two CHMs shows that the canopy height has increased by about 5 m in the period from 2000 to 2006.

4.2. Determination of aerodynamic roughness for momentum transport

The aerodynamic roughness parameters estimated using the spatial averages of λ and h for each CHM are listed against the adopted method in Table 4. The computed ratios z_0/h and d_0/h are also listed in the table. The results show that the selected methods produce widely differing estimates. The figures of Table 4 were compared with published mean values of z_0/h and d_0/h obtained from different studies. Since the published z_0 and d_0 values fall into a wide range of canopy heights, it is sensible to compare the normalized height values. The published mean values of z_0/h and d_0/h are respectively 0.076 and 0.78 (Garratt, 1992) and therefore, the results of Grant and Mason (1990) model are in good agreement with these values for the TLS data. Similarly, Kutzbach (1961) and Raupach (1992) have produced d_0/h estimates fairly consistent with the corresponding mean value. However, the z_0/h and d_0/h values predicted by the Raupach (1994) model are further away from the published mean values of Garratt (1992).

In the present analysis we assumed parameter values $z_{01} = 0.01$ m and $c_{d0} = 0.3$ in the Grant and Mason (1990) model to estimate z_0 of the canopy surface. It is reported that previous studies have used the model with slightly different values; $c_{d0} = 0.4$ (Menenti and Ritchie, 1994) and c_{d0} around 0.75–1.0 (Hiyama et al., 1996) to calculate z_0 in different landscapes. The estimated z_0 value is rather sensitive to the choice of c_{d0}. For instance, changing c_{d0} from 0.3 to 0.5 would increase z_0 from 1.6 m to 2.6 m. Nevertheless, a value between 0.3 and 0.4 for c_{d0} yields z_0 estimates that are comparable with the published values.

Both the Raupach (1992, 1994) models contain a number of parameters viz. C_S, C_R, c, c_w, c_d, and c_{d1} introduced during the formulation. The recommended values for C_R, and c_w have been deduced from theory while others were determined empirically. Since the parameters have been originally calibrated using relatively closed canopies ($\lambda > 0.5$) their applicability to sparser canopies is doubtful. Verhoef et al. (1997) have evaluated

Table 5
Comparison of model parameters in Raupach (1992, 1994) models.

Parameter	Original values	Verhoef et al. (1997) values		Proposed values
		For z_0	For d_0	
Raupach (1992)				
C_R	0.3	0.42	0.47	0.42
C_S	0.003	0.01	0.01	0.01
c	0.37	−1.30	−3.80	0.37
c_d	0.60	0.20	0.20	0.60
Raupach (1994)				
C_R	0.3	0.35	0.35	0.35
C_S	0.003	0.01	0.01	0.01
c_{d1}	15	20.6	21	45

Raupach's models comparing the model predictions against published values of aerodynamic roughness parameters determined from wind profile measurements. These authors have adopted a value of $C_S = 0.01$ from literature considering the type of vegetation (shrubs). They determined values for C_R, c and c_{d1} which were quite different from the original values given by Raupach (1992, 1994). They have further emphasized that with the new optimized parameters Raupach's models perform better for a wide range of canopies varying in density from closed to sparse. The values reported by Verhoef et al. (1997) for Raupach's models are listed in Table 5.

It was observed that both the Raupach (1992, 1994) models perform better with the modified parameters of Verhoef et al. (1997). However the use of different values for parameters C_R (0.42 and 0.47) and c (−1.3 and −3.8) to estimate z_0 and d_0 respectively in the Raupach (1992) model (see Table 5) by Verhoef et al. (1997) seems to be unrealistic. In order to avoid that, we proposed a new set of parameters. We observed that much better results can then be obtained. It was also observed that parameter c_{d1} can be changed to obtain results much closer to the published mean values reported for coniferous forests (Garratt, 1992). The final proposed model parameters are listed in Table 5.

We carried out a sensitivity analysis to find out the impact of varying the average λ on our resulted aerodynamic parameters using adopted methods. The variation of d_0 and z_0 predicted by different models with respect to λ is illustrated in Fig. 9. The results indicate that the estimated z_0 using the Grant and Mason (1990) model is much more sensitive to λ compared to the other two models.

Table 6
Estimated roughness parameters using proposed model parameters.

Model	Average from TLS		Average from ALS	
	z_0 (m)	z_0/h	z_0 (m)	z_0/h
Raupach (1992)	1.678	0.065	1.341	0.064
Raupach (1994)	1.721	0.067	1.354	0.064
Model	Average from TLS		Average from ALS	
	d_0 (m)	d_0/h	d_0 (m)	d_0/h
Raupach (1992)	19.56	0.758	14.64	0.694
Raupach (1994)	19.96	0.773	14.93	0.708

5. Derivation of effective height using area–height relationship of CHM

5.1. Representation of roughness elements using basic geometric shapes

Leonard and Federer (1972) estimated roughness parameters of a red pine plantation using a contour map of the upper canopy surface. They derived the surface parameters based on the assumption that the canopy can be represented by an array of uniform obstacles such as cones or paraboloids (of height h^*) having tangent bases in either square or hexagonal close packing. The fractional surface area (α) for a three dimensional object with a given packing geometry can be defined as the vertically projected surface area above a given height (z) per unit circumscribed area of the regular polygon. Accordingly α for a surface modelled by the cone is given as:

$$\alpha = \frac{\pi}{4}\left(1 - \frac{z - d_0}{h^*}\right)^2 \quad \text{(for square packing)} \tag{10}$$

$$\alpha = \frac{\pi}{2\sqrt{3}}\left(1 - \frac{z - d_0}{h^*}\right)^2 \quad \text{(for hexagonal packing)} \tag{11}$$

and for the paraboloid is given as

$$\alpha = \frac{\pi}{4}\left(1 - \frac{z - d_0}{h^*}\right) \quad \text{(for square packing)} \tag{12}$$

$$\alpha = \frac{\pi}{2\sqrt{3}}\left(1 - \frac{z - d_0}{h^*}\right) \quad \text{(for hexagonal packing)} \tag{13}$$

The above set of equations can be derived using the algebraic relations of the surface geometry of a cone or a paraboloid of height

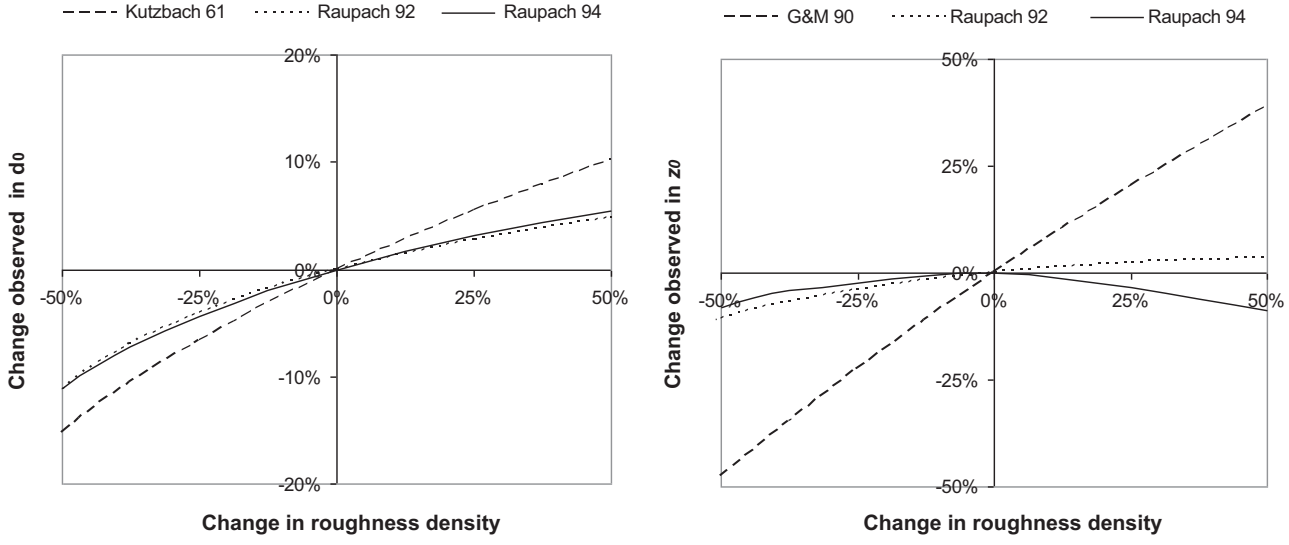

Fig. 9. Sensitivity of d_0 and z_0 estimated from different models with respect to λ.

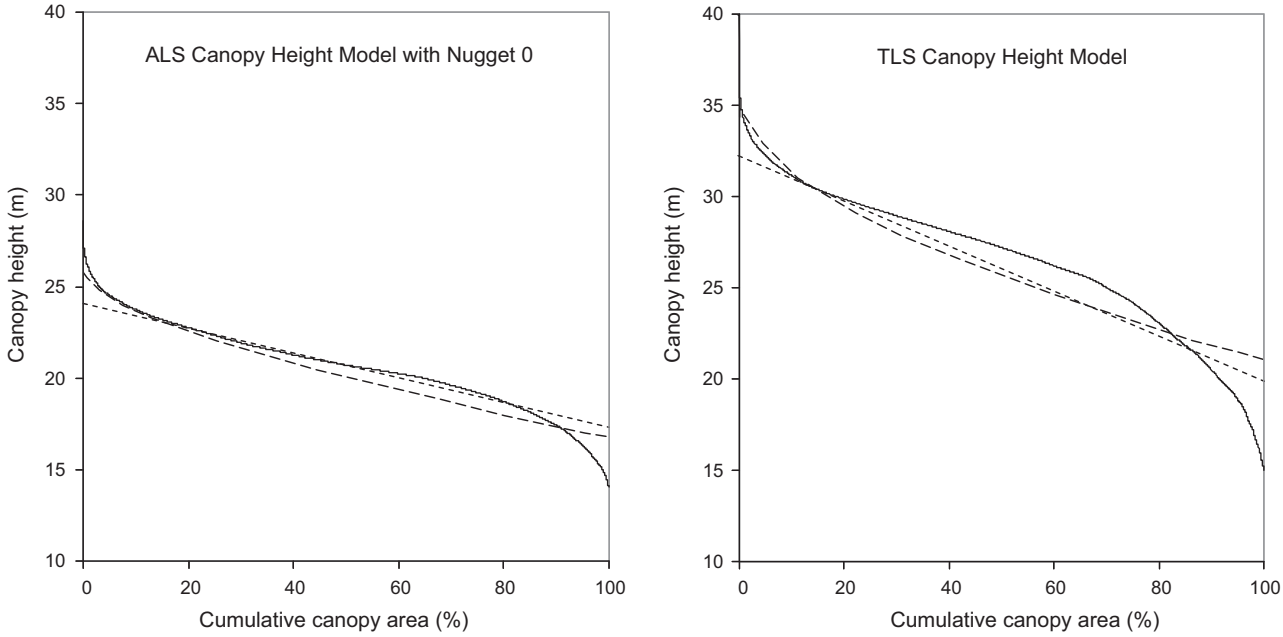

Fig. 10. Area height relationship of the CHM showing the fitted geometrical models. The solid lines show the values obtained from the canopy height models. Short dashed lines indicate the paraboloid model. Long dashed lines indicate the conical model.

h^* in connection with the respective close packing geometry at the base, as described by Leonard and Federer (1972). Height h^* corresponds to the height of the cone or paraboloid above the displacement height d_0. Height z is measured above the surface level. It should be noted that the maximum α for square packing is $\pi/4$ (Eqs. (10) and (12)) whereas the maximum α for hexagonal packing is $\pi/(2\sqrt{3})$ (Eqs. (11) and (13)).

5.2. Determination of d_0 and h^* using cumulative area–height relationship

Using the ALS and TLS canopy height models generated previously, we obtained the cumulative area–height relationships (graph of cumulative α versus height) of the forest canopy (see Fig. 10). With this relationship it is possible to derive values for d_0 and h^* by means of Eqs. (10)–(13). One of the options is by fitting the equations at two arbitrary points of the area–height relationship and solving for d_0 and h^*. Leonard and Federer (1972) used two fixed α values at 0.15 and 0.85 (15 and 85%) to obtain two canopy intercepts, which allowed them to solve the Eqs. (10)–(13) for h^* and d_0. (see Tables 7 and 8). Alternatively solutions for d_0 can be found by considering the fact that α reaches its maximum value ($\alpha = \pi/4$ for square packing and $\alpha = \pi/(2\sqrt{3})$ for hexagonal packing) when z is equal to d_0. In this case the value of d_0 depends only on the packing geometry and the assumed shape is irrelevant. The second point can be taken at $\alpha = 0.15$ as in the case of Leonard and Federer (1972) to solve for h^*. The resulted values for h^* and d_0 for two options are summarized in Tables 7 and 8 and some solution are illustrated in Fig. 10.

In accordance with Thom (1971) and De Bruin and Moore (1985), z_0 can be assumed proportional to h^*

$$z_0 = \mu h^* \tag{14}$$

where μ is an empirical coefficient around 0.2–0.3.

The observed canopy height distribution of the area represented by CHM is near normal as shown by the *S*-shaped curves of Fig. 10. It is evident that neither cone nor paraboloid model is perfectly matching the cumulative area height relationship of the two CHMs. Although the cone seems to be fitting the upper 10% of the canopy surface (canopy heights above 32 m for TLS and same above 24 m for ALS), overall fit is slightly better with the paraboloid shape. This is further illustrated in Fig. 11 by comparing the modelled cone and the paraboloid shapes against TLS point data over a typical crown section. It is also evident from the comparison that the assumed shapes and packing geometry reasonably fit the TLS data.

The results obtained using the method described in Section 5.2 are listed in Tables 7 and 8. Although the estimated values of d_0 are fairly consistent with the assumed shape and the packing geometry, the estimated h^* and thus the z_0 estimates differ depending on the assumed shape and packing. Obviously the value of z_0 depends on the choice of the μ value too. De Bruin and Moore (1985) have found $\mu = 0.22$ for a pine forest using anemometric methods. We observed that (with a value for $\mu = 0.2$) the estimated d_0 and z_0 values for the paraboloid shapes are in good agreement with the

Table 7
Results obtained with different geometrical models after fitting the TLS-CHM.

TLS ($\mu = 0.2$)				
Shape	Packing	h^* (m)	d_0 (m)	z_0 (m)
Cone	Square	13.752	22.345	2.750
Cone	Hexagonal	17.058	19.967	3.412
Cone	Hexagonal (15–85)	15.888	20.661	3.178
Paraboloid	Square	9.570	22.345	1.914
Paraboloid	Hexagonal	12.126	19.967	2.425
Paraboloid	Hexagonal (15–85)	11.557	20.443	2.311

Table 8
Results obtained with different geometrical models after fitting the ALS-CHM.

ALS ($\mu = 0.2$)				
Shape	Packing	h^* (m)	d_0 (m)	z_0 (m)
Cone	Square	5.772	19.431	1.154
Cone	Hexagonal	7.525	18.216	1.505
Cone	Hexagonal (15–85)	6.747	18.677	1.349
Paraboloid	Square	4.017	19.431	0.803
Paraboloid	Hexagonal	5.349	18.216	1.070
Paraboloid	Hexagonal (15–85)	4.908	18.584	0.982

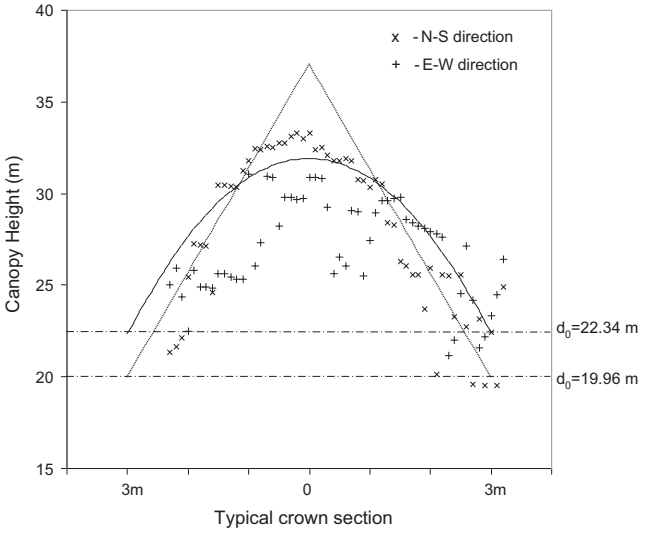

Fig. 11. A typical crown section fitted with cone in hexagonal packing and paraboloid in square packing shapes. TLS point data for two principal directions are compared.

values of Table 6 for the TLS image, while agreement for the ALS image is better for the model with the conical shapes. However, the agreement between the results of Sections 4 and 5 is fair, considering the large variation in z_0 values between different types of land surface and vegetation cover.

6. Conclusions

In this study we used high resolution laser scans to construct digital canopy height models of a coniferous forest. We explored the use of these height models to estimate aerodynamic roughness parameters of the forest stand. We tested several morphometric models, based on the theories of Kutzbach (1961), Grant and Mason (1990) and Raupach (1992, 1994). The models basically used the obstacle density as the independent variable to estimate roughness parameters.

The estimated average obstacle density was in the range of 0.14–0.24 in both canopy height models. The estimated average λ values depend very much on the selected moving average filter size. Nevertheless the highest estimated λ values (without applying a moving average) are within the range of values reported for similar land surfaces. For different canopy types, Verhoef et al. (1997) have reported a range of λ from 0.04 (Vineyard) to 0.6 (Savannah) citing several references. Our estimated λ values suggest that we are in the category of relatively sparse canopies ($\lambda < 0.5$). It should be noted that the results indicate that roughness density of the forest has increased in the period of six years between the ALS and TLS measurements.

The results show that z_0 and d_0 of a tall vegetation canopy can be satisfactorily determined through the laser derived surface features. The results also show that the Raupach models perform better with the optimized parameters recommended by Verhoef et al. (1997). Although the models of Grant and Mason (1990) and Kutzbach (1961) produced reasonable estimates of z_0 and d_0 in this study, their applicability to higher roughness densities is doubtful. Nevertheless Raupach models with parameters tuned to resemble the forest structure of the study area can be applied to a wide range of roughness densities.

The cumulative area–height modelling produced results which are compatible with other models. This approach is particularly useful because a smaller number of empirical constants is needed in comparison to the former models. However, knowledge of μ is important as it significantly affects the z_0 estimate. Our results have shown that, to model the upper canopy surface of the coniferous forest, both the cone and the paraboloid shapes are fairly appropriate. However with present results we are unable to clearly establish the fact that one model is favoured over the other to employ with either TLS or ALS method. Usually a scanner that is more likely to miss the tree apexes (this is common with TLS due to occlusion and wind effect) may favour the use of paraboloid model. Also with ALS method, tree tops are likely to be missed as a consequence of the under-sampling and this may particularly affect coniferous trees such as fir or spruce. Therefore when extrapolating these methods to large areas with different canopy geometries one has to accommodate these limitations. Further our assumption of having an impenetrable upper canopy surface is arbitrary and unrealistic since most of the forest canopies naturally act as permeable surfaces. Many studies in the field of fluid mechanics have indicated that the velocity profiles over permeable surfaces are more turbulent than those over impermeable rough surfaces. This has been attributed to the additional energy dissipation caused by exchange of momentum across the permeable surface. In consequence of the above assumption it is more likely that we have underestimated the forest aerodynamic roughness. As a final remark we would mention that the results of the present study can be compared with roughness parameters estimated with aerodynamic methods using on-site turbulence or wind profile measurements. This will be dealt with in a forthcoming study.

Acknowledgements

This work was funded in part by EU GMES EAGLE Project (FP6, SST3 – CT – 2003 – 502057), NWO/SRON EO-071 and ESA EAGLE2006 (EOP-SM/1504/RB-dr). The TLS measurements were made by FUGRO Inpark B.V. We thank Erik Claassen, for data pre-processing and Patrick van Laake, Zoltan Verkerdy, Joris Timmermans, Ron Rezema and Remco Dost for their contribution in TLS data acquisitions. We also thank Gerard Reinink for facilitating to obtain ALS data from the ITC database.

References

Bosveld, F.C., 1999. Exchange processes between a coniferous forest and the atmosphere. Ph.D. Thesis, Wageningen University, The Netherlands, 181 pp.
Brutsaert, W., 1982. Evaporation into the Atmosphere. Reidel Publishing Co., Dordrecht, Holland, 299 pp.
Burden, R.L., Faires, J.D., 2010. Numerical Analysis, 9th ed. PWS Publishers, 872 pp.
Colin, J., Faivre, R., 2010. Aerodynamic roughness length estimation from very high-resolution imaging LIDAR observations over the Heihe basin in China. Hydrol. Earth Syst. Sci. 7, 3397–3421.
De Bruin, H.A.R., Moore, C.J., 1985. Zero-plane displacement and roughness length for tall vegetation, derived from a simple mass conservation hypothesis. Bound. Lay. Meteorol. 31, 39–49.
De Vries, A.C., Kustas, W.P., Ritchie, J.C., Klaassen, W., Menenti, M., Rango, A., Prueger, J.H., 2003. Effective aerodynamic roughness estimated from airborne laser altimeter measurements of surface features. Int. J. Remote Sens. 24 (7), 1545–1558.
Dorsey, J.R., Duyzer, J.H., Gallagher, M.W., Coe, H., Pilegaard, K., Weststrate, J.H., Jensen, N.O., Walton, S., 2004. Oxidized nitrogen and ozone interaction with forests. I: experimental observations and analysis of exchange with Douglas fir. Quart. J. Roy. Meteorol. Soc. 130, 1941–1955.
EEA, 1992. CORINE Land Cover, A European Community Project, European Environment Agency Task-Force, Directorate General for the Environment, Nuclear Safety and Civil Protection. Commission of the European Communities.
Garratt, J.R., 1992. The Atmospheric Boundary Layer. Cambridge University Press, 316 pp.
Grant, A.L.M., Mason, P.J., 1990. Observations of boundary-layer structure over. complex terrain. Quart. J. Roy. Meteorol. Soc. 116, 159–186.
Grimmond, C.S.B., Oke, T.R., 1999. Aerodynamic properties of urban areas derived from analysis of surface form. J. Appl. Meteorol. 38, 1262–1292.
Hasager, C.B., Nielsen, N.W., Jensen, N.O., Boegh, E., Christensen, J.H., Dellwik, E., Soegaard, H., 2003. Effective roughness calculated from satellite-derived land cover maps and hedge-information used in a weather forecasting model. Bound. Lay. Meteorol. 109, 227–254.
Hiyama, T., Sugita, M., Kotoda, K., 1996. Regional roughness parameters and momentum fluxes over a complex area. J. Appl. Meteorol. 35, 2179–2190.

Hollaus, M., Wagner, W., Eberhofer, C., Karel, W., 2006. Accuracy of large-scale canopy heights derived from LiDAR data under operational constraints in a complex alpine environment. J. Photogramm. Remote Sens. 60, 323–338.

Jasinski, M.F., Crago, R.D., 1999. Estimation of vegetation aerodynamic roughness of natural regions using frontal area density determined from satellite imagery. Agric. For. Meteor. 94, 65–77.

Kutzbach, J., 1961, Investigations of the modification of wind profiles by artificially controlled surface roughness. Annual Report, Department of Meteorology, University of Wisconsin-Madison.

Leonard, R.E., Federer, C.A., 1972. Estimated and measured roughness parameters for a pine forest. J. Appl. Meteorol. 12, 302–307.

Mason, P.J., 1985. On the parameterization of orographic drag. In physical parameterization for numerical models of the atmosphere. In: E.C.M.W.F., Reading Seminar, 9–13 September, 1985, pp. 139–167.

Menenti, M., Ritchie, J.C., 1994. Estimation of effective aerodynamic roughness of alnut Gulch watershed with laser altimeter data. Water Resour. Res. 30, 1329–1337.

Raupach, M.R., 1992. Drag and drag partition on rough surfaces. Bound. Lay. Meteorol. 60, 375–395.

Raupach, M.R., 1994. Simplified expressions for vegetation roughness length and zero-plane displacement as functions of canopy height and area index. Bound. Lay. Meteorol. 71, 211–216.

Raupach, M.R., 1995. Corrigenda. Bound. Lay. Meteorol. 76, 303–304.

Su, Z., Timmermans, W.J., van der Tol, C., Dost, R., Bianchi, R., Gómez, J.A., House, A., Hajnsek, I., Menenti, M., Magliulo, V., Esposito, M., Haarbrink, R., Bosveld, F., Rothe, R., Baltink, H.K., Vekerdy, Z., Sobrino, J.A., Timmermans, J., van Laake, P., Salama, S., van der Kwast, H., Claassen, E., Stolk, A., Jia, L., Moors, E., Hartogensis, O., Gillespie, A., 2009. EAGLE 2006 – multi-purpose, multi-angle and multi-sensor insitu and airborne campaigns over grassland and forest. Hydrol. Earth Syst. Sci. 13, 833–845.

Stull, R.B., 1988. An introduction to Boundary Layer Meteorology. Kluwer Academic Publishers, Dordrecht, 666 pp.

Thom, A.S., 1971. Momentum absorption by vegetation. Quat. J. Roy. Meteorol. Soc. 97, 414–428.

Van Heerd, R.M., Kuijlaars, E.A.C., Teeuw, M.P., van't Zand, R.J., 2000. Productspecificatie AHN 2000 (Rijkswaterstaat—Adviesdienst Geo-informatie en ICT, Report MDTGM 2000.13). Available online at: http://www.ahn.nl.

Van der Tol, C., van der Tol, S., Verhoef, A., Su, Z., Timmermans, J., Houldcroft, C., Gieske, A.S.M., 2009. A Bayesian approach to estimate sensible and latent heat over vegetated land surface. Hydrol. Earth Syst. Sci. 13, 749–758.

Verhoef, A., McNaughton, K.G., Jacobs, A.F.G., 1997. A parameterization of momentum roughness length and displacement height for a wide range of canopy densities. Hydrol. Earth Syst. Sci. 1, 81–91.